Fishnet Metamaterials - Rules for Refraction and Limits of Homogenization

L. Jelinek[1*], R. Marques[2] and J. Machac[1]

[1]*Department of Electromagnetic Field, Czech Technical University in Prague, 16627 Prague (Czech Republic)*
[2]*Department of Electronics and Electromagnetism, University of Seville, Avd. Reina Mercedes, 41012 Sevilla (Spain)*
[*]*jelinek@us.es*

Abstract: The perfectly conducting stacked fishnet metamaterial is studied in this paper. The analysis is based on a combination of the mode matching method together with the generalized eigenvalue problem, and takes into account wave propagation along all three Cartesian axes. The analysis has been developed for a fishnet of square lateral periodicity and for two particular polarizations, namely TE and TM, corresponding to the two most common excitations. The 1D and 2D dispersion characteristics are calculated for both polarizations, showing that the TM waves undergo negative refraction in a narrow frequency band just below Wood's anomaly, whereas TE polarized waves exhibit ordinary positive refraction. Finally, possible homogenization of the fishnet metamaterial is considered, showing that only for small angles of incidence and in the immediate vicinity of Wood's anomaly can the fishnet be seen as homogenizable uniaxial medium.

OCIS codes: (160.3918) Metamaterials; (050.2065) Effective medium theory; (160.1245) Artificially engineered materials; (160.5298) Photonic crystals

References and links

1. S. Zhang, W. Fan, K. J. Malloy, and S. R. J. Brueck, "Near-infrared double negative metamaterials," Opt. Express **13**, 4922-4929 (2005).
2. S. Zhang, W. Fan, N. C. Panoiu, K. J. Malloy, R. M. Osgood, and S. R. J. Brueck, "Experimental Demonstration of Near-Infrared Negative-Index Metamaterials," Phys. Rev. Lett. **95**, 137404 (2005).
3. G. Dolling, Ch. Enkrich, M. Wegener, C. M. Soukoulis, and S. Linden, "Low-loss negative-index metamaterial at telecommunication wavelengths," Opt. Lett. **31**, 1800-1802 (2005).
4. M. Beruete, M. Sorolla, and I. Campillo, "Left-handed extraordinary optical transmission through a photonic crystal of subwavelength hole arrays," Opt. Express **14**, 5445-5455 (2006).
5. G. Dolling, M. Wegener, C. M. Soukoulis, and S. Linden, "Negative-index metamaterial at 780 nm wavelength," Opt. Lett. **32**, 53-55 (2007).
6. M. Beruete, I. Campillo, M. Navarro-Cia, F. Falcone, and M.S. Ayza, "Molding left- or right-handed metamaterials by stacked cutoff metallic hole arrays," IEEE Trans. Antennas Propag. **55**, 1514-1521 (2007).
7. M. Navarro-Cia, M. Beruete, M. Sorolla, and I. Campillo, "Negative refraction in a prism made of stacked subwavelength hole arrays," Opt. Express **16**, 560-566 (2008).
8. J. Valentine, S. Zhang, T. Zentgraf, E. Ulin-Avila1, D. A. Genov1, G. Bartal, and X. Zhang, "Three-dimensional optical metamaterial with a negative refractive index," Nature (London) **455**, 376-379 (2008).
9. A. Mary, S. G. Rodrigo, F. J. Garcia-Vidal, and L. Martin-Moreno, "Theory of negative-refractive-index response of double-fishnet structures," Phys. Rev. Lett. **101**, 103902 (2008).

#130205 - $15.00 USD Received 15 Jun 2010; revised 21 Jul 2010; accepted 26 Jul 2010; published 5 Aug 2010

10. M. Beruete, M. Navarro-Cia, M. Sorolla, and I. Campillo, "Negative refraction through an extraordinary transmission left-handed metamaterial slab," Phys. Rev. B **79**, 195107 (2009).
11. R. Marques, L. Jelinek, F. Mesa, and F. Medina, "Analytical theory of wave propagation through stacked Fishnet metamaterials," Opt. Express **17**, 11582-11593 (2009).
12. R. Marques, F. Mesa, L. Jelinek, and F. Medina, "Analytical theory of extraordinary transmission through metallic diffraction screens perforated by small holes," Opt. Express **17**, 5571-5579 (2009).
13. C. Menzel, T. Paul, C. Rockstuhl, T. Pertsch, S. Tretyakov, and F. Lederer, "Validity of effective material parameters for optical fishnet metamaterials," Phys. Rev. B **81**, 035320 (2010).
14. M. Beruete, M. Navarro-Cia and M. Sorolla, "Strong lateral displacement in polarization anisotropic extraordinary transmission metamaterial," New J. of Phys. **12**, 063037 (2010).
15. C. Garcia-Meca, R. Ortuno, F. J. Rodriguez-Fortuno, J. Marti, and A. Martinez, "Negative refractive index metamaterials aided by extraordinary optical transmission," Opt. Express **17**, 6026-6031 (2009).
16. L. D. Landau, E. M. Lifshitz and L. P. Pitaevskii, *Electrodynamics of Continuous Media*, 2nd ed. (Pergamon Press, New York, 1984).

1. Introduction

Fishnet metamaterials made of a stack of two or more metallic plates perforated by small holes have been extensively studied in recent years [1] – [11]. In these works, the negative refractive index (extracted from an analysis of the transmission and reflection coefficients for normally incident plane waves), as well as backward-wave propagation inside the stack, have been extensively studied, both theoretically and experimentally. Recently, negative refraction at the exit interface of a prism made of a fishnet metamaterial has been shown experimentally at microwaves [7] and at optical frequencies [8]. Even more recently, negative refraction at the flat interface of a fishnet stack was predicted in [9] and experimentally shown in [10]. All this theoretical analysis and experimental evidence, together with the simplicity of the design, form the basis of the present interest in metamaterial structures of this kind.

In a recent paper, some of the authors [11] developed an analytical solution for normal wave propagation inside an infinite stack of perfectly conducting metallic fishnets. This analysis was, in fact, a generalization of a previous analysis of extraordinary transmission through single fishnets [12], which took advantage of the equivalence between this last problem and the problem of a plane discontinuity in a TEM waveguide. The analysis provided evidence of a close relation between wave propagation in stacked fishnets and extraordinary optical transmission, something already reported in [4] and [9]. In particular, it was shown that in small hole stacked fishnets, there is always a backward transmission band ending at Wood's anomaly, the bandwidth of which increases with the hole size and decreases with the periodicity of the stack. For bigger holes, this band becomes forward (now starting at Wood's anomaly), and additional forward bands related to the hole resonance may appear. In this paper, this analysis is generalized to account for wave propagation along directions different from the normal to the stack. The band diagram and the iso-frequency contours of the stacked fishnet are calculated, and from this analysis the conditions for negative and positive refraction at the fishnet interface are identified. Finally, the possibilities and limits for homogenization of the structure, a question that has been recently raised [13], are discussed. It has to be noted that during the review process the paper [14] appeared reaching similar conclusions.

2. Analysis

A sketch of the unit cell of the analyzed structure is shown in Fig. 1a,b. Fishnets are stacked along the z-direction and the structure is defined by the dimensions of the rectangular window w_x, w_y, the lateral periodicities p_1, p_2, the longitudinal periodicity p_3, and the diaphragm thickness t. The metallic structure is immersed in a host material with permittivity ε_{h} and permeability μ_{h}.

#130205 - $15.00 USD Received 15 Jun 2010; revised 21 Jul 2010; accepted 26 Jul 2010; published 5 Aug 2010

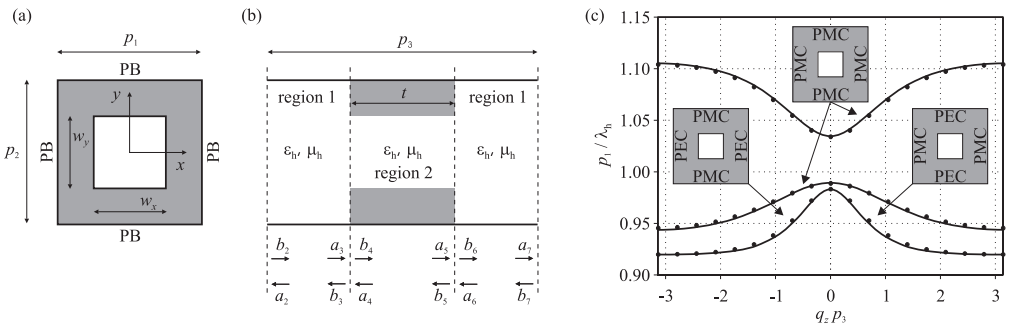

Fig. 1. Panels (a) and (b) show the front and side view of the analyzed unit cell. Panel (c) shows the dispersion diagram for normal incidence on a structure with $p_1 = p_2$, $w_x = w_y = p_1/3$, $p_3 = p_1/9$, $t = p_1/30$ and some host material (lines come from the presented method, while dots come from CST). The lateral boundaries are indicated in all the panels and are either a periodic boundary (PB), a perfect magnetic conductor (PMC) or a perfect electric conductor (PEC). The gray regions in all the panels represent a perfect electric conductor.

The analysis is based on the mode-matching solution of the scattering problem with mode coefficients a_3, b_3, a_4, b_4 (see Fig. 1b), with the scattering matrices

$$\begin{aligned} \mathbf{b}_3 &= \bar{\mathbf{s}}_{11}\mathbf{a}_3 + \bar{\mathbf{s}}_{12}\mathbf{a}_4 \\ \mathbf{b}_4 &= \bar{\mathbf{s}}_{21}\mathbf{a}_3 + \bar{\mathbf{s}}_{22}\mathbf{a}_4 \end{aligned} \tag{1}$$

which relate the vectors of the coefficients of the modal expansions on both sides of the discontinuity. After some algebra, the following relation can be obtained:

$$\begin{aligned} \mathbf{a}_2 &= \left\{\bar{\mathbf{L}}_1^+ \bar{\mathbf{x}}_{11} \bar{\mathbf{L}}_1^+\right\}\mathbf{b}_2 + \left\{\bar{\mathbf{L}}_1^+ \bar{\mathbf{x}}_{12} \bar{\mathbf{L}}_1^+\right\}\mathbf{b}_7 \\ \mathbf{a}_7 &= \left\{\bar{\mathbf{L}}_1^+ \bar{\mathbf{x}}_{21} \bar{\mathbf{L}}_1^+\right\}\mathbf{b}_2 + \left\{\bar{\mathbf{L}}_1^+ \bar{\mathbf{x}}_{22} \bar{\mathbf{L}}_1^+\right\}\mathbf{b}_7, \end{aligned} \tag{2}$$

where

$$\bar{\mathbf{x}} = \begin{bmatrix} \bar{\mathbf{s}}_{11} + \bar{\mathbf{s}}_{12}\bar{\mathbf{L}}_2^+ \bar{\mathbf{s}}_{22}\bar{\mathbf{x}}_2 \bar{\mathbf{L}}_2^+ \bar{\mathbf{s}}_{21} & \bar{\mathbf{s}}_{12}\bar{\mathbf{L}}_2^+ \left(\bar{\mathbf{s}}_{22}\bar{\mathbf{x}}_2\bar{\mathbf{x}}_1\bar{\mathbf{s}}_{21} + \bar{\mathbf{s}}_{21}\right) \\ \bar{\mathbf{s}}_{12}\bar{\mathbf{x}}_2\bar{\mathbf{L}}_2^+\bar{\mathbf{s}}_{21} & \bar{\mathbf{s}}_{12}\bar{\mathbf{x}}_2\bar{\mathbf{x}}_1\bar{\mathbf{s}}_{21} + \bar{\mathbf{s}}_{11} \end{bmatrix} \tag{3}$$

and

$$\begin{aligned} \bar{\mathbf{L}}_1^+ &= \mathrm{diag}\left[e^{-\mathrm{j}k_{z1}(p_3-t)/2}\right] \\ \bar{\mathbf{L}}_2^+ &= \mathrm{diag}\left[e^{-\mathrm{j}k_{z2}t}\right] \\ \bar{\mathbf{x}}_1 &= \bar{\mathbf{L}}_2^+ \bar{\mathbf{s}}_{22} \bar{\mathbf{L}}_2^+ \\ \bar{\mathbf{x}}_2 &= \left\{\bar{\mathbf{1}} - \bar{\mathbf{x}}_1\bar{\mathbf{s}}_{22}\right\}^{-1}. \end{aligned} \tag{4}$$

In (4), the wavenumbers of internal waveguide modes in region 1 and 2, respectively, are defined as (see Fig. 1a,b)

$$\begin{aligned} k_{z1}^2 &= \varepsilon_h\mu_h\left(\frac{\omega}{c_0}\right)^2 + \left(\frac{2m\pi}{p_1} + q_x\right)^2 + \left(\frac{2n\pi}{p_2} + q_y\right)^2 \;;\; m = -M..M,\; n = -N..N \\ k_{z2}^2 &= \varepsilon_h\mu_h\left(\frac{\omega}{c_0}\right)^2 + \left(\frac{r\pi}{w_x}\right)^2 + \left(\frac{s\pi}{w_y}\right)^2 \;;\; r = 0..R,\; s = 0..S. \end{aligned} \tag{5}$$

#130205 - $15.00 USD Received 15 Jun 2010; revised 21 Jul 2010; accepted 26 Jul 2010; published 5 Aug 2010

The matrices in (2) connecting the vector coefficients $\mathbf{a}_2$, $\mathbf{b}_2$, $\mathbf{a}_7$, $\mathbf{b}_7$ are just the s-matrices of the complete structure $\overline{\mathbf{s}}_{11}^{\text{tot}}, \overline{\mathbf{s}}_{12}^{\text{tot}}, \overline{\mathbf{s}}_{21}^{\text{tot}}, \overline{\mathbf{s}}_{22}^{\text{tot}}$ and from knowing them we can finally formulate the eigenvalue problem for the stack of fishnets by imposing the periodic boundary conditions

$$\begin{aligned} \mathbf{a}_7 &= e^{-\mathrm{j}q_z p_3}\mathbf{b}_2 \\ \mathbf{b}_7 &= e^{-\mathrm{j}q_z p_3}\mathbf{a}_2 \end{aligned} \tag{6}$$

which leads to the generalized eigenvalue problem for the longitudinal wavenumber q_z

$$\begin{bmatrix} \overline{\mathbf{1}} & -\overline{\mathbf{s}}_{11}^{\text{tot}} \\ \overline{\mathbf{0}} & -\overline{\mathbf{s}}_{21}^{\text{tot}} \end{bmatrix} \begin{bmatrix} \mathbf{a}_2 \\ \mathbf{b}_2 \end{bmatrix} = e^{-\mathrm{j}q_z p_3} \begin{bmatrix} \overline{\mathbf{s}}_{12}^{\text{tot}} & \overline{\mathbf{0}} \\ \overline{\mathbf{s}}_{22}^{\text{tot}} & -\overline{\mathbf{1}} \end{bmatrix} \begin{bmatrix} \mathbf{a}_2 \\ \mathbf{b}_2 \end{bmatrix} \tag{7}$$

which is solved by generalized QR decomposition. Lateral wavenumbers q_x and q_y are introduced in the analysis as parameters by specific shape of internal waveguide modes and wavenumbers k_{z1} and k_{z2}, see (5).

Even though the above mentioned method can be theoretically used for lossy metals (for example metals at optical frequencies), all the results presented in this paper will be shown for the perfect conducting metal approximation. The inclusion of metal losses would be accompanied by severe complications in construction of proper waveguide modes for the mode-matching technique. In the practical case, where penetration depth in the metal is finite but still small in comparison to the structural parameters, all the qualitative results presented later will however be valid and the difficulties in theoretical analysis will not be counterbalanced by improvement of the insight into the fishnet structures.

In order to check the validity of our method, several numerical simulations of band diagrams have been carried out by using the CST Microwave studio commercial electromagnetic solver. For comparison, a general rectangular periodicity and hole was chosen. Excellent agreement between our method and the commercial solver was observed in the whole range of q_x, q_y and q_z. An example of the comparison can be found in Fig. 1 and Fig. 2.

3. Propagation along Cartesian axes

Before we move to the issue of refraction, the fishnet will be first analyzed in the case of propagation along the Cartesian axes, starting from propagation along the z-axis, that is for $q_x = 0$, $q_y = 0$ (normal incidence). The dispersion diagram is shown in Fig. 1c for some representative structural parameters [8, 15]. Figure 1c shows three passbands in the depicted frequency range, with a stopband at lower frequencies. At first sight it seems that the propagation is multimodal and thus inconsistent with the approximation by effective homogeneous medium. However, an examination of the field distribution corresponding to the three dispersion branches reveals that the 2$^{\text{nd}}$ and 3$^{\text{rd}}$ branches (from the bottom) are compatible with PMC x- and y-sidewalls and are thus not compatible with excitation of the fishnet by a normally incident plane wave. The 1$^{\text{st}}$ branch corresponds to two degenerated modes, one of them with PEC x-sidewalls and PMC y-sidewalls, and the second one with these walls interchanged. These two modes correspond to some normally incident E_x and E_y polarized plane waves that are degenerated for a square hole and periodicity. Therefore, excitation by a plane wave at normal incidence prevents multimodal propagation, being thus compatible with homogenization. The frequency range of interest has an upper limit given by the top point of the 1$^{\text{st}}$ mode in Fig. 1c, characterized by $p_1/\lambda_{\text{h}} \approx 0.984$, where λ_{h} is the wavelength in the host material.

Let us now consider oblique incidence. Starting from a normally incident plane wave polarized with the electric field along the y-axis, and varying the angle of incidence in the $y-z$ plane, we obtain the waves characterized by wavenumbers $q_x = 0, q_y \neq 0, q_z \neq 0$ and magnetic x-sidewalls in Fig. 1a. We will call these waves TM modes, because they correspond to a TM

#130205 - $15.00 USD Received 15 Jun 2010; revised 21 Jul 2010; accepted 26 Jul 2010; published 5 Aug 2010

incident plane wave with field components E_y, E_z, H_x impinging on the fishnet. If, starting from the same normally incident wave, we vary the angle of incidence in the $x-z$ plane, we obtain waves characterized by $q_x \neq 0, q_y = 0, q_z \neq 0$ and electric *y*-sidewalls. We will call these waves TE modes, because they correspond to a TE incident plane wave with field components E_y, H_x, H_z. Note that the above mentioned TM and TE modes are not, strictly speaking, TE and TM polarized modes inside the metamaterial. These denominations only denote the "dominant" polarization, and the fact that they can be excited by incident TM and TE plane waves, respectively. As will become apparent later, most relevant information about the behavior of fishnet metamaterials can be extracted from an analysis of these TM and TE polarizations.

Considering TM modes with $q_z = q_x = 0$ we obtain waves propagating along the *y*-axis, whose dispersion diagram is shown in Fig. 2a. As is shown in the Figure, these TM modes mainly propagate along the light lines with $q_y = k_\mathrm{h} \pm 2\pi/p_2 = 2\pi/\lambda_\mathrm{h} \pm 2\pi/p_2$. This fact can be easily interpreted as the propagation of an almost TEM plane wave (with the electric field polarized along the *z* axis) between the parallel plate waveguides formed by the fishnets. This behavior only changes near Wood's anomaly, as a consequence of the interaction with the holes. Conversely, for TE modes with $q_z = q_y = 0$, the above mentioned parallel plate waveguides are below cutoff for frequencies below Wood's anomaly, and these modes cannot propagate. Thus, the propagation of TE modes with $q_z = 0$ is only possible at frequencies around Wood's anomaly and above, as shown in Fig. 2b.

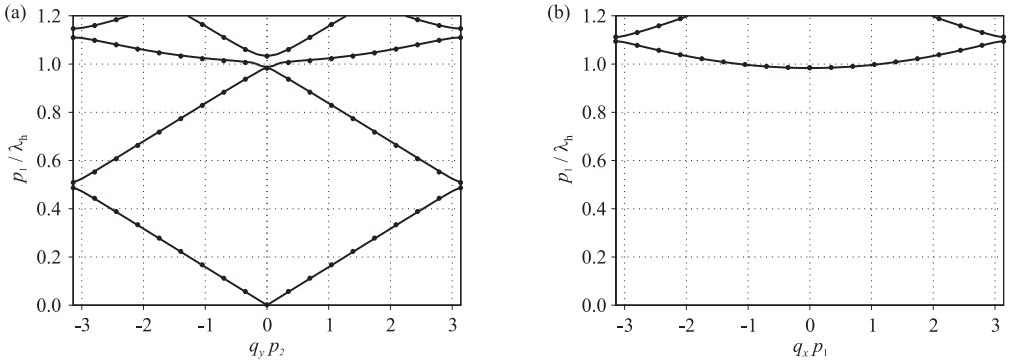

Fig. 2. Band diagram cut for $q_z = q_x = 0$ corresponding to the TM case (a) and band diagram for $q_z = q_y = 0$ corresponding to the TE case (b). The structural parameters are identical with Fig. 1c. The lines come from the presented method, while dots come from CST.

Although Fig. 1c and Fig. 2 show only cuts of the complete dispersion diagram, they actually show all the most important features of the complete band diagram. In fact, the general shape of the dispersion along q_z must be conserved for all the values of q_x and q_y. Moreover - owing to the square periodicity of the fishnets - the band diagrams for $q_z = q_y = 0$ and for $q_z = q_x = 0$ for the TM and TE polarizations, respectively, must coincide with those shown in Fig. 2 for the orthogonal directions in **q**-space.

4. Iso-frequency contours and negative refraction

In order to study refraction properties, the iso-frequency contours of the above mentioned TM and TE modes have been analyzed. The results of this analysis are shown in Figs. 3 and 4. The TM modes will be analyzed first. Figure 3 shows that, in the frequency range of interest (close to Wood's anomaly, but below $p_1/\lambda_\mathrm{h} \approx 0.984$), TM modes have two branches (here we have considered all modes with $q_x = 0, q_y \neq 0, q_z \neq 0$ and magnetic *x*-sidewalls in Fig. 1a, regardless

#130205 - $15.00 USD Received 15 Jun 2010; revised 21 Jul 2010; accepted 26 Jul 2010; published 5 Aug 2010

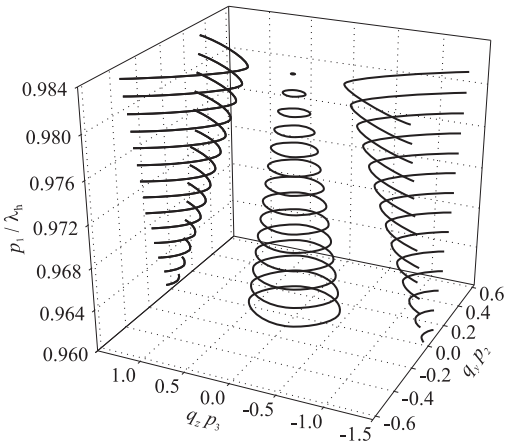

Fig. 3. Iso-frequency contours for TM polarization. The structural parameters are the same as in Fig. 1c.

of its mechanism of excitation). The first branch forms an elliptical cone and corresponds to the extension of the 1st mode in Fig. 1c to non-zero values of q_y. The second branch forms the two hyperbolic surfaces shown in Fig. 2a, and corresponds to the extension of the 2nd mode in Fig. 1c to non-zero values of q_y. As was discussed in Sec. 3., the hyperbolic mode cannot be excited by a normally incident plane wave, but for oblique incidence it can. However, if we restrict ourselves to wavenumbers limited by the condition (note that $q_x = 0$ for TM polarization and $q_y = 0$ for TE polarization)

$$|q_x \cdot p_1|^2 + |q_y \cdot p_2|^2 + |q_z \cdot p_3|^2 < (\pi/5)^2, \tag{8}$$

i.e. to wavenumbers small enough to allow for homogenization (periodicity smaller than $\lambda/10$ [13]), the hyperbolic surface disappears and the fishnet can be treated as a single mode structure. For this case, the iso-frequency contours of the TM modes are shown again in Fig. 4a. They form quasi-elliptical curves, which reduce to a single point around $p_1/\lambda_h \approx 0.984$, which is the frequency where the 1st mode of Fig. 1c reaches its maximum. Let us now consider a plane wave with a wave-vector $\mathbf{k}$ incident from the semi-space $z < 0$ on the interface (at $z = 0$) of a semi-infinite stacked fishnet metamaterial. The wave-vector $\mathbf{q}$ of the refracted wave is determined by the continuity of the tangential component at the interface ($q_y = k_y$) and by energy conservation: energy must flow into the fishnet. Taking into account that the direction of the group velocity must coincide with the gradient of the iso-frequency contours, the wave will exhibit negative refraction, as is graphically shown in Fig. 5.

Let us now consider the TE modes. In this case the propagation is always single modal, with the quasi-hyperbolic iso-frequency contours shown in Fig. 4b. The refraction of a plane wave incident at an oblique angle over the fishnet interface can be analyzed in the same way as for the TM modes. Here, however, the refracted energy points into the same side of the normal as the wave vector of the incident wave. Therefore, TE polarized plane waves will exhibit positive refraction, which is in agreement with previously published observations [6].

5. Homogenization

At first sight, Fig. 4 shows that the frequency region of possible homogenization (restricted by (8)) is different for the TM case and for the TE case. Particularly, the allowed frequency band for TM polarization goes from $p_1/\lambda_h \approx 0.900$ to $p_1/\lambda_h \approx 0.984$, while the allowed frequency band

#130205 - $15.00 USD Received 15 Jun 2010; revised 21 Jul 2010; accepted 26 Jul 2010; published 5 Aug 2010

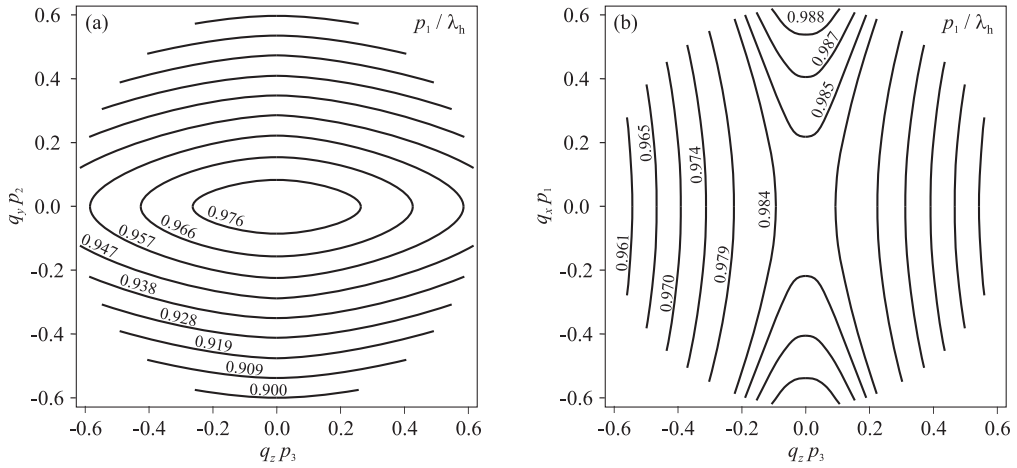

Fig. 4. Iso-frequency contours for (a) TM and (b) TE polarization. The structural parameters are the same as in Fig. 1c. The interval of allowed **q** is restricted by (8).

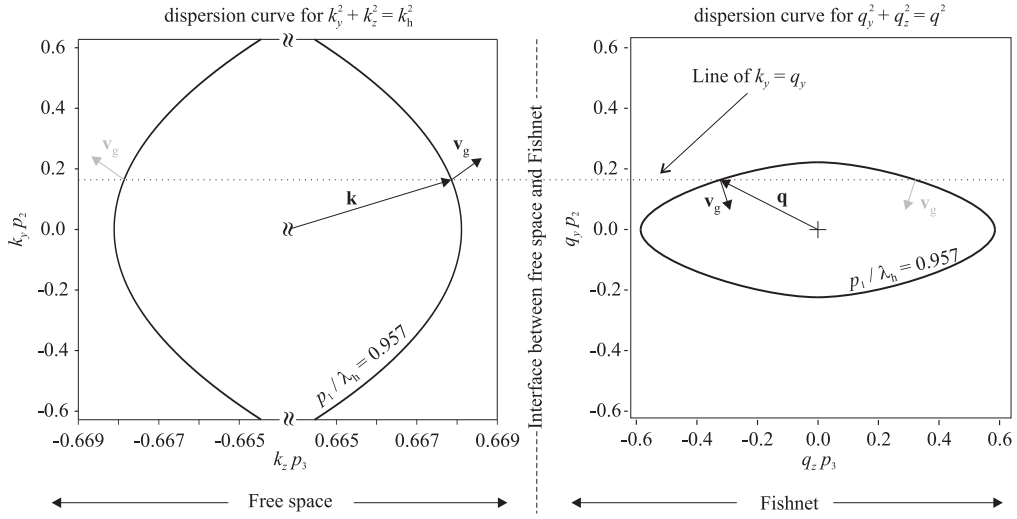

Fig. 5. Graphical representation of TM polarized plane wave refraction on the planar boundary between free space and fishnet. Group velocity is signed as $\mathbf{v}_g$, with black arrows corresponding to the waves propagating along the *z*-axis and gray arrows corresponding to the waves in the opposite direction. Note that the phase velocity in *z* direction $v_{fz} = \omega/k_z$ or $v_{fz} = \omega/q_z$ is positive for the wave on the left panel and negative for the right panel.

for TE polarization goes from $p_1/\lambda_h \approx 0.961$ to $p_1/\lambda_h \approx 0.984$ (it should be noted, however, that if one wants to see the fishnet as a homogeneous medium, then homogenization has to be possible for both polarizations simultaneously, and in such a case the allowed frequency band of TE polarization has to be used). Taking into account that the angle of the incident plane wave is $\sin(\theta_i) = q_\perp/k_0$ (where $q_\perp$ accounts for q_x or q_y), the above conditions allow only angles $\sin(\theta_i) \lesssim n_h/9$ for TM and $\sin(\theta_i) \lesssim n_h/10$ for TE polarization, with n_h being the refractive index of the host material. For higher angles of incidence, the homogenizable TE and TM modes cannot be excited in the metamaterial.

#130205 - $15.00 USD Received 15 Jun 2010; revised 21 Jul 2010; accepted 26 Jul 2010; published 5 Aug 2010

The iso-frequency contours in Fig. 4 seem to have the shape of some quadratic curves and therefore, taking into account the rotational symmetry of the structure, the dispersion equation for TE and TM polarization can, in the above frequency ranges, be approximated as

$$q_z^2 = n^2 k_0^2 + r q_\perp^2, \tag{9}$$

where n^2 and r are some frequency dependent parameters (of course r takes different values for TE and TM modes). In the limit $q_\perp \to 0$, this dispersion relation reads $q_z = nk_0$ and therefore n must be identified with the refractive index extracted from the analysis of transmission and reflection under normal incidence. According to Fig. 1c, k_0 and q_z must have opposite signs for normal incidence and therefore $n < 0$, in agreement with previously published results. Since the iso-frequency curves are ellipses (hyperbolas) for TM (TE) waves, it should be $r^{\mathrm{TM}} < 0$ ($r^{\mathrm{TE}} > 0$). The values of the aforementioned parameters for the analyzed structure are shown in Fig. 6 and come from the least-squares fitting of the dispersion equation (9) to the contours in Fig. 4. Note that in order to keep the analysis independent of the host material, the index of refraction has been normalized to the refractive index of the host medium. That is, the actual refractive index of the fishnet is given by $n = n_0 \cdot n_{\mathrm{h}}$, where n_0 corresponds to the fishent filled with a vacuum and n_{h} is the refractive index of the host.

Two important conclusions can be drawn from Fig. 6. First, the values of n_0^{TM} and n_0^{TE} are similar (in the common frequency range), but not identical as they should be in a real medium (for normal incidence the TM and TE polarizations are identical). The difference between them reflects the fact that the dispersion equation (9) cannot fit the real dispersion exactly. Therefore, this difference corresponds to the error associated to the homogeneous medium approximation. The second conclusion apparent from Fig. 6 is that the negative refractive index for normal incidence n is not sufficient to characterize - even approximately - the behavior of the fishnet for angles of incidence other than zero, however small they may be.

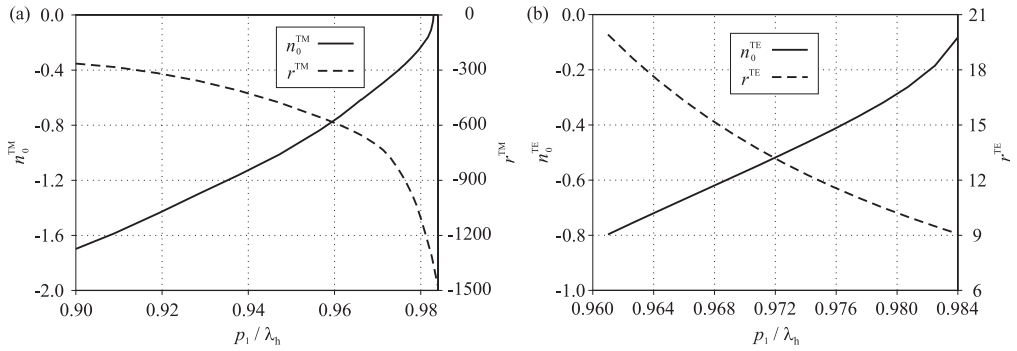

Fig. 6. Least-square fitted parameters n_0^{TM}, n_0^{TM}, r^{TE}, and r^{TE} corresponding to (9). The structural parameters are the same as in Fig. 1c.

Strictly speaking, our analysis is only valid for propagation in the planes $q_x = 0$ or $q_y = 0$ of the **q**-space. However, as far as the transverse wavelength $\lambda_\perp = 2\pi/\sqrt{q_x^2 + q_y^2}$ is large with regard to the transverse periodicity $p_1 = p_2$, it can be guessed that the dispersion equation for the two propagating eigenmodes will still be described by (9) for all values of $q_\perp$. This behavior is typical for a uniaxial magneto-dielectric crystal with its main axis oriented perpendicular to the interface. In fact, the only difference between this magneto-dielectric crystal and an ordinary uniaxial dielectric medium is the presence of two extraordinary waves instead of a single wave (for ordinary uniaxial dielectric media it is $r^{TE} = 0$ [16]). Thus, assuming an external beam

#130205 - $15.00 USD Received 15 Jun 2010; revised 21 Jul 2010; accepted 26 Jul 2010; published 5 Aug 2010

impinging over the flat interface $z = 0$ of the metamaterial at an oblique angle, the angle of refraction of energy is defined by $\tan(\theta_r) = S_\perp / S_z$, where $S_\perp$ and S_z are the components of the Poynting vector. For TM and TE waves propagating in these uniaxial magneto-dielectric crystals, this ratio can be written as

$$\tan(\theta_r) = \frac{S_\perp}{S_z} = -r\,\frac{q_\perp}{q_z}, \tag{10}$$

where $r = r^{TM}$ ($r = r^{TE}$) for TM (TE) polarization. Assuming a positive angle of incidence $\theta_i > 0$, it must be also $q_\perp = k_0 \sin(\theta_i) > 0$. On the other hand, since propagation along the normal is always backward, it must be $q_z < 0$. It therefore follows from the signs of r^{TM} and r^{TE} that the angle of refraction must be negative for TM waves and positive for TE waves, in agreement with the results of Sec. 4. Actually, from (9), (10) and $q_\perp = k_0 \sin(\theta_i)$ it follows that

$$\sin^2(\theta_r) = \frac{r^2 \sin^2(\theta_i)}{n^2 + (r^2 + r)\sin^2(\theta_i)}, \tag{11}$$

which is valid for both TE and TM waves and generalizes Snell's law. As can be seen, this expression only reduces to Snell's law for the specific case of $r = -1$, which is far from being fulfilled in the analyzed structure. The numerical values coming from (11) are plotted in Fig. 7.

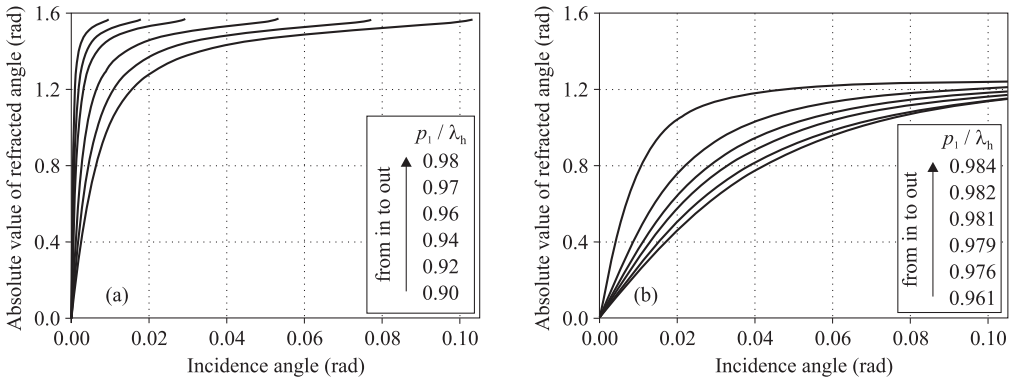

Fig. 7. Refraction angle versus incidence angle and frequency for (a) TM polarization and (b) TE polarization. The $n_{\mathrm{h}} = 1$ is assumed. As input data the curves from Fig. 6 have been used. Note that (11) only gives absolute value of refraction angle, however, using (10) the negative sign has to be assigned to TM case, while positive sign has to be assigned to TE case.

6. Conclusions

Perfectly conducting fishnet metamaterials have been analyzed using a combination of the mode matching method and generalized eigenmode analysis. The analysis was developed for TM and TE polarized plane waves impinging on the fishnet, which represents the most common excitation used in the literature. For both cases, 1D dispersion diagrams and 2D isofrequency dispersion plots have been obtained. Our analysis shows that, in general, fishnet metamaterials present multimode propagation. However, for small transverse wavenumbers and in the vicinity of Wood's anomaly, fishnet metamaterials show unimodal propagation. It follows from the analysis of this monomode propagation that TM plane waves impinging at small angles over the outer fishnet interface experience negative refraction, whereas TE plane waves show positive

#130205 - $15.00 USD Received 15 Jun 2010; revised 21 Jul 2010; accepted 26 Jul 2010; published 5 Aug 2010

refraction. Along with the rules for refraction, the possible homogenization of fishnet metamaterials has been studied. It has been shown that the frequency region of possible homogenization is different for TM and TE modes, and that the homogenization of a fishnet is mainly limited by TE polarization. In both cases, homogenization is restricted to a narrow frequency band below Wood's anomaly, and to the incident waves within a small apex angle cone. Under such restrictions, the fishnet has been shown to behave like an uniaxial magneto-dielectric medium with the main axis lying along the normal to the fishnet planes. Snell's law for refraction at the fishnet interface (parallel to the fishnet planes) has been generalized as a function of the homogenized parameters of the fishnet, n, r^{TE} and r^{TM}, defined in this paper. It follows from this analysis that the index of refraction extracted from normal incidence analysis is far from being sufficient for characterizing - even approximately - the refraction phenomenon in these structures. We feel that the analysis reported here is useful for clarifying the rules of refraction at fishnet metamaterial interfaces. It also helps to a better understanding of the scope and limits of fishnet homogenization, providing a theoretical framework for such homogenization when it is possible.

Acknowledgments

This work has been supported by the Spanish Ministerio de Educación y Ciencia and European Union FEDER funds (projects TEC2007-65376, TEC2007-68013-C02-01, and CSD2008-00066), by Junta de Andalucía (project TIC-253), by the Czech Grant Agency (project no. 102/09/0314), and by the Czech Technical University in Prague (project no. SGS10/271/OHK3/3T/13).

#130205 - $15.00 USD Received 15 Jun 2010; revised 21 Jul 2010; accepted 26 Jul 2010; published 5 Aug 2010